Composites Part B 98 (2016) 56–69

Contents lists available at ScienceDirect

Composites Part B

journal homepage: www.elsevier.com/locate/compositesb

Bond mechanism and bond strength of GFRP bars to concrete: A review

Fei Yan, Zhibin Lin*, Mijia Yang

Department of Civil and Environmental Engineering, North Dakota State University, Fargo, ND 58018-6050, USA

ARTICLE INFO

Article history:
Received 13 March 2016
Received in revised form
22 April 2016
Accepted 25 April 2016
Available online 10 May 2016

Keywords:
B. Fiber/matrix bond
A. Glass fibers
B. Environmental degradation
A. Polymer-matrix composites (PMCs)
C. Statistical properties/methods

ABSTRACT

Glass fiber-reinforced polymer (GFRP) reinforcements are taken as an alternative solution for the deterioration of civil infrastructures. GFRP bars have received increasing attention due to low cost compared to carbon fiber-reinforced polymer (CFRP) bars. Bond characteristic of GFRP bars in concrete is the most critical parameter for implementation of the material to the corrosion-free concrete structures. Unlike steel reinforcement, GFRP materials behave anisotropic, non-homogeneous and linear elastic properties, which may result in different force transfer mechanism between reinforcement and concrete. With the purpose of covering the most valuable contributions regarding bond mechanism in the past work, a comprehensive review focusing on the failure mode and bond strength is carried out in this paper. A database consisted of 682 pullout-test specimens was created to observe the factors affecting bond behavior. Basic relationship between bond strength/slip and factors was analyzed accordingly. In addition, the development of bond degradation under environmental conditions, such as freezing-thawing cycling, wet-dry cycling, alkaline solutions and high temperature was presented thereafter. These environmental influences need to be further investigated.

1. Introduction

Corrosion of steel reinforcing bars in reinforced concrete (RC) structures is a serious problem when they are in exposure to various environments [1]. In particular, sodium chloride and calcium chloride based deicers, traditionally used in cold regions for snow and ice removal operations, primarily respond for the initiation of steel corrosion. Corrosion process and its products damage the interface between steel bar and concrete, thus degrade bond strength, and ultimately shorten the service life of the concrete structures. This arises up to substantial economic burden during periodic maintenance, repairs and rehabilitations in the United States, Canada and European countries [2–4]. There has been an increasing demand for alternate materials and techniques for reinforcement in RC structures [5–7]. These include coating techniques (fusion bonded epoxy and galvanized coatings) on steel or non-metallic reinforcements (carbon fiber-reinforced polymer, glass fiber-reinforced polymer and aramid fiber-reinforced polymer). Among them GFRP reinforcing bar has received increasing attention due to its high chemical resistance, high strength-weight ratio, and high cost efficiency, as well as its superior corrosion resistance [8].

Bond characteristics of GFRP bars in concrete are the most critical parameter for implementation of the material to the concrete structures. Unlike steel reinforcement, GFRP materials behave anisotropic, non-homogeneous and linear elastic properties, which results in different force transfer mechanism between reinforcement and concrete. Primary factors affecting bond behavior [9–12], such as concrete strength, concrete cover, and concrete confinement provided by transverse reinforcement, have been investigated based on either beam test or direct pullout test [13–18]. Correspondingly, design codes for FRP reinforcement in the U.S., Canada and Japan have stipulated guidelines associated with bond mechanism in terms of both embedment length and bond strength [1,19–21].

Although much research has showed that different factors respond for the different bond performance of GFRP bars in concrete and accordingly yield the different bond strength, current design codes cannot accurately account for the bond strength with respect to transverse reinforcement. For example, the empirical bond strength equations used in ACI 440.1R-06 (2012) is defined based on Wambeke and Shield [22] database, of which very few of

* Corresponding author. Tel.: +1 701 231 7204; fax: +1 701 231 6185.
E-mail address: zhibin.lin@ndsu.edu (Z. Lin).

http://dx.doi.org/10.1016/j.compositesb.2016.04.068
1359-8368/

the beam test specimens encompassed transverse reinforcement. On the other hand, several models have been developed to construct the bond stress-slip relations [23–25] and each of them may be derived under certain assumptions. So far, no unified model is available that can be applied to general bond behavior of GFRP bar. Thus it is necessary to review the existing bond models and their applicability, for assisting engineers to select desirable models.

Moreover, since concrete has a high alkaline with a pH value ranging from 12.7 to 13.6 [26,27], several previous studies demonstrated that GFRP bars embedded in concrete have reduction in both tensile and bond strengths [28–32]. Laboratory based tests also revealed that elevated temperature can further accelerate their strength degradation process [33]. Degradation modeling and prediction (e.g., Arrhenius concept) of tensile strength retention has been proposed and been successfully validated [26,32]. Bond degradation of GFRP bars in concrete, however, in particular under harsh environments, such as extremely thermal cycling, alkaline solutions and other chemical attacks, is more complex, while accordingly existing studies and methods on mechanism and prediction are different and even in contrary opinions in the available literature [34–36]. Thus, it is important to better understand their bond behavior and mechanism for more widespread applications of GFRP bars in concrete structures.

To maximize the knowledge and experience gained in existing studies and practices in the literature, this study is undertaken to summarize the key issues primarily on bond mechanism in terms of failure modes and bond strength. Both bond stress vs. slip models and primary factors affecting bond behavior are investigated through statistical analysis based on a database created. Meanwhile, comparisons between different design standards regarding bond strength prediction are presented and discussed in this study. Furthermore, bond degradations under environmental conditions, such as freezing-thawing cycling, wet-dry cycling, alkaline solutions and high temperature are presented and analyzed respectively. Future work for both theoretical bond degradation and laboratory test would be performed based on the contribution covered in this study.

2. Bond behavior and modeling of GFRP bars to concrete

2.1. Bond stress-slip behavior and its modeling

Generally, bond of reinforcing bar to concrete includes: a) Adhesion resistance of the interface, defined as chemical bond; b) Frictional resistance of the interface against slip; and c) Mechanical interlock due to irregularity of the interface [37]. GFRP bar has a different bond behavior compared to steel bar, which is mainly attributed to difference in material property and surface texture that lead to different surface toughness and the force transfer mechanism between reinforcement and concrete [13,38,39]. GFRP reinforcement behaves linearly elastic till failure, whereas conventional steel reinforcement exhibits an obvious plastic stage with large deformation after yielding. GFRP bar usually has different surface texture and treatments, such as ribbed, sand coated and helically wrapped, and thus its bearing force due to mechanical interlock is commonly smaller than that of steel ribbed bar. It is believed that such mechanical interlock of surface texture and surface treatments to concrete matrix accounts for the majority of bond strength of GFRP bar over chemical adhesion or friction [11]. However, another contrary opinion holds that chemical adhesion is the primary bond during pullout process, while mechanical interlock and friction are only the secondary contribution [40].

Currently, several analytical models of bond stress vs. slip relations have been developed using the explicit mathematical formula to describe bond behavior of FRP bar to concrete, as addressed in the following sections.

2.1.1. BPE and modified BPE models

The BPE model was originally developed to describe bond behavior of steel bar to concrete [41], as shown in Fig. 1. Consider that the FRP bond has no apparent plateau as steel bar, the model was then modified as Fig. 2 for FRP material [39]. In this model, the bond-slip curve of the FRP bar in concrete, illustrated in Fig. 2, is mainly simplified into three stages. In stage I, an ascending function in bond stress corresponds to the chemical adhesion between the bar and concrete, as well as the bearing force. Cracks develop at later this stage. After the bond force increases to a certain value, the bar starts to slide along the lug area. Concrete cracks (or even crushing) occur and the bearing force due to mechanical interlocking against the concrete diminishes, resulting in a rapid decrease of the bond stress accompanying with an apparent slip as shown in stage II. In stage III, significant cracks formed in the concrete and the bar continues to slide while remaining a certain bond force mainly due to friction.

Thus, the modified BPE (mBPE) bond stress-slip model in Fig. 2 can be piecewisely expressed as these three stages in Eqns. (1a)–(1c).

$$\frac{\tau}{\tau_b} = \left(\frac{s}{s_b}\right)^{\alpha} \text{ for } 0 \le s \le s_b, \tag{1a}$$

$$\frac{\tau}{\tau_b} = 1 - p\left(\frac{s}{s_b}\right) \text{ for } s_b \le s \le s_3, \tag{1b}$$

$$\tau = \tau_3 \text{ for } s \ge s_3, \tag{1c}$$

where τ and s are defined as the bond stress and the slip, while τ_b and s_b are the maximum bond stress (bond strength) and its corresponding slip; α and p are parameters that can be determined from curve fitting of experimental results. The effect of surface treatment on bond strength is considered in this model [36]. The ascending branch of BPE/mBPE was observed to have larger bond stress than the experimental results in Masmoudi's work. It is worth noting that both fiber type and bar diameter are not taken into account in this model.

2.1.2. Malvar's model

Rather than use of three piecewise equations in the mBPE model [36], this model uses a polynomial function [42] to predict the bond stress-slip behavior, as shown below in Eqn. (2a):

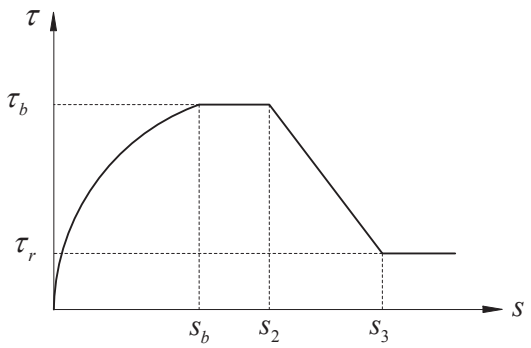

Fig. 1. BPE model for steel bar.

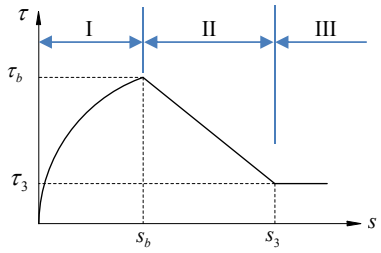

Fig. 2. Modified BPE model for FRP bar.

$$\tau = \tau_b \frac{F\left(\frac{s}{s_b}\right) + (G-1)\left(\frac{s}{s_b}\right)^2}{1 + (F-2)\frac{s}{s_b} + G\left(\frac{s}{s_b}\right)^2}, \tag{2a}$$

where,

$$\frac{\tau_b}{f_t} = A + B\left(1 - e^{-C\sigma_r/f_t}\right) \text{ and } s_b = D + E\sigma_r, \tag{2b}$$

in which constants A, B, C, D, E, F and G are parameters to be determined from experimental results; σ_r is confining axisymmetric radial pressure while f_t is concrete tensile strength.

In Malvar's study [39], GFRP bar with four different surface textures were investigated. Note that Malvar's model did not predict the first ascending stage as accurately as the mBPE model [39]. Moreover, it is assessed to be less reliable compared to BPE, mBPE and CMR models [43]. Additionally, impacts of bar diameter on the bond strength were ignored in this model.

2.1.3. CMR model

To overcome the drawback of the Malvar's model, the CMR model proposed by Cosenza et al. [44] was used to better represent ascending function at the first stage of bond stress-slip curve for FRP bar to concrete in form of.

$$\frac{\tau}{\tau_b} = \left(1 - exp\left(-\frac{s}{s_r}\right)\right)^{\beta}, \tag{3}$$

where s_r and β are parameters that are derived from curve fitting of experimental data. Since the initial slope in the CMR model is infinite, it may account for impacts of chemical adhesion at the initial stage. It shows a good agreement with experimental results than the BPE model in Masmoudi's study.

2.1.4. Parameters determined for the existing bond-slip models

As compared to the mBPE model and the CMR model, Malvar's model requires more parameters to be determined and has been reported to be less comprehensive and lower reliable [43]. Differently, the mBPE model and CMR model are more concise and convenient for implementation and thus these two models will be mainly discussed herein. Basically, α in the mBPE model in Eqn. (1a), and s_r and β in the CMR model in Eqn. (3) are determined using the data-driven curve fitting.

The data reported in Refs. [24,25,45–47] were used to demonstrate the distribution state of the fitting parameters. Those test contained the parameters including the bar size, surface treatment, concrete compressive strength, kinds of fibers, kinds of test, operating temperature. Data from literature in terms of the bar size and surface treatment are plotted in Fig. 3, in which parameters α, s_r and β are displayed by squares, circles and triangles, respectively. High variation in Fig. 3 revealed that values of these parameters in the mBPE and CMR models are highly affected by different rebar conditions, such as rebar diameter and surface treatment [25,45–47], and other environmental factors, such as varying operating temperature [24]. For GFRP rebars with a diameter of 12.7 mm and with a surface of helically wrapped and sand coated, $\alpha = 0.18$ was suggested for mBPE model, and $s_r = 0.0668$, and $\beta = 0.3691$ for CMR model [47]. Yoo et al. (2015) calibrated parameters in the existing models for GFRP rebar with different diameters. Specifically, for diameter of 12.7 mm, the coefficients of mBPE model has $\alpha = 0.18$; while $s_r = 0.16$, and $\beta = 0.50$ for CMR model. In addition, Masmoudi et al. (2011) investigated the impacts of elevated temperature on the selection of parameters. Their tests for GFRP rebars with a 16-mm diameter after 4 months thermal exposure showed that the parameter α is likely a constant, with 0.085 at 20 °C, 0.089 at 40 °C, 0.087 at 60 °C and 0.084 at 80 °C.

The box plots for these three parameters with regard to specific rebar diameter and surface treatment are displayed in Figs. 4 through 6. The lower and upper limits in these plots can provide a preference of parameters to a certain extent if when experiments are not available. For example, α is supposed to be the median that can be derived from the left boxplot of Fig. 4, when diameter is equal to 12.7 mm, α is found to be 0.2715, and similarity to β and s_r. With the obtained parameters for either the mBPE or CMR, the bond-slip model of GFRP rebar to concrete will be available.

2.2. Bond strength specified in existing design provisions

2.2.1. ACI 440.1R-06

Bond strength of FRP bar to concrete is specified in ACI 440.1R-06 [1], a linear regression of normalized average bond stress $(\tau_b/\sqrt{f'_c})$ is described by the normalized concrete cover (c/d_b) and embedment length (l_d/d_b):

$$\frac{\tau_b}{0.083\sqrt{f'_c}} = 4.0 + 0.3\frac{C}{d_b} + 100\frac{d_b}{l_d}, \tag{4}$$

where τ_b is the bond strength (MPa); f'_c is the concrete compressive strength (MPa) at 28-day age; c is the lesser of the cover to the center of the bar or one-half of the center-on-center spacing of the bars being developed; d_b is bar diameter; l_d is embedded length in concrete. This equation was developed from a comprehensive study by Wambeke and Shield [22] through the 269 bond tests. The tests built up a valuable database, widely covering beam-end tests, notch-beam tests, and splice tests, while GFRP bars were used as the major reinforcement (by 240 out of total number of 269). Bar surfaces included sand coated, spiral wrap and helical lug, including with and without confining reinforcements. The diameter of the bar ranged from 13 to 29 mm. The concrete compressive strength ranged from 28 to 45 MPa. Out of 240 GFRP specimens, 75 failed by concrete splitting, 94 by pullout failure and 71 by bar tensile fracture failure. In the Wambeke and Shield database, the bar surface did not appear to influence the test results. Meanwhile, no explicit expression was presented to the transverse reinforcement, however it was claimed that the confinement influence needs to be further investigated.

2.2.2. Canadian Standards Association

Canadian Standards Association (CSA S806-02) [20] specifies the following equation for the average bond strength of FRP bars to concrete:

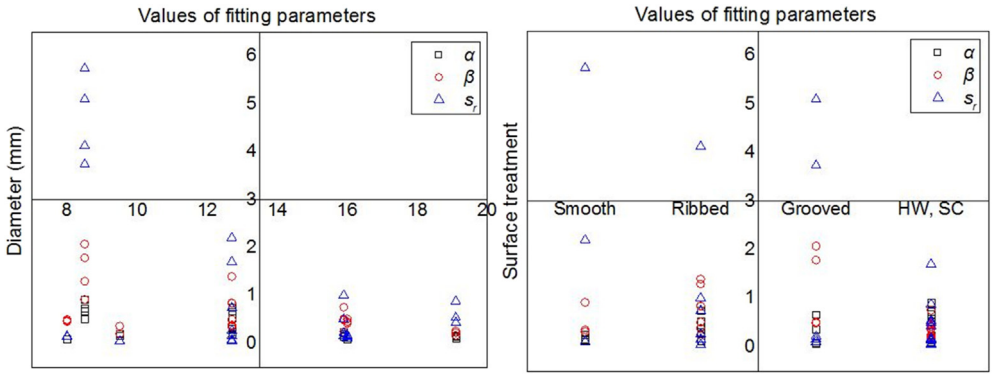

Fig. 3. Dispersion conditions of fitting parameters β and s_r.

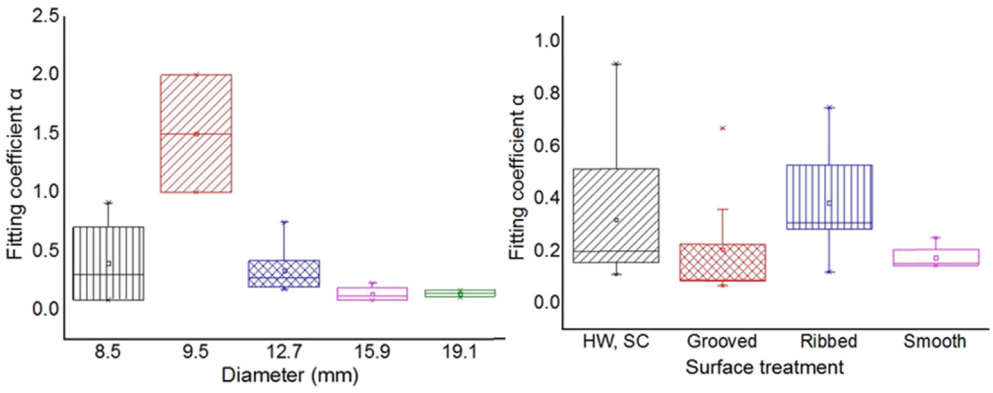

Fig. 4. Discrete conditions of fitting parameter α.

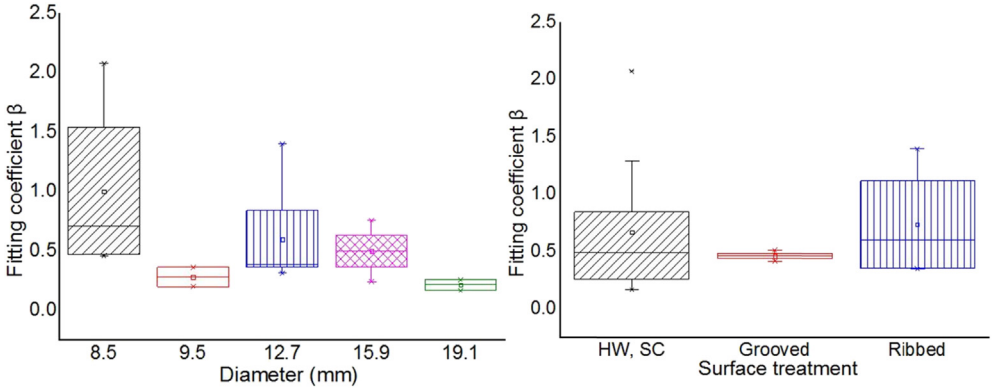

Fig. 5. Discrete conditions of fitting parameter β.

$$\tau_b = \frac{d_{cs}\sqrt{f'_c}}{1.15(K_1K_2K_3K_4K_5)\pi d_b}, \tag{5}$$

where d_{cs} is the smallest of the distance from the closest concrete surface to the center of the bar being developed or two-thirds the center-on-center spacing of the bars being developed (mm); K_1 is bar location factor (1.3 for horizontal reinforcement placed more than 300 mm of fresh concrete is cast below the bar, 1.0 for all other cases); K_2 is concrete density factor (1.3 for structural low-density concrete, 1.2 for structural semi-low-density concrete, 1.0 for normal-density concrete); K_3 is bar size factor (0.8 for $A_b \leq 300$ mm^2, 1.0 for $A_b > 300$ mm^2); K_4 is bar fiber factor (1.0 for CFRP and GFRP, 1.25 for AFRP); K_5 is bar surface profile factor (1.0 for surface roughened or sand coated or braided surfaces, 1.05 for spiral pattern surfaces or ribbed surfaces, 1.8 for indented surfaces). Thus, it can be observed that the proposed bond strength in Eqn. (5) corresponds to concrete cover, concrete strength, concrete density, bar diameter, bar surface conditions, bar location, and fiber type.

2.2.3. Canadian Highway Bridge Design Code

Canadian Highway Bridge Design Code (CSA S6-06) [21] recommends the bond strength of FRP bars to concrete in the following:

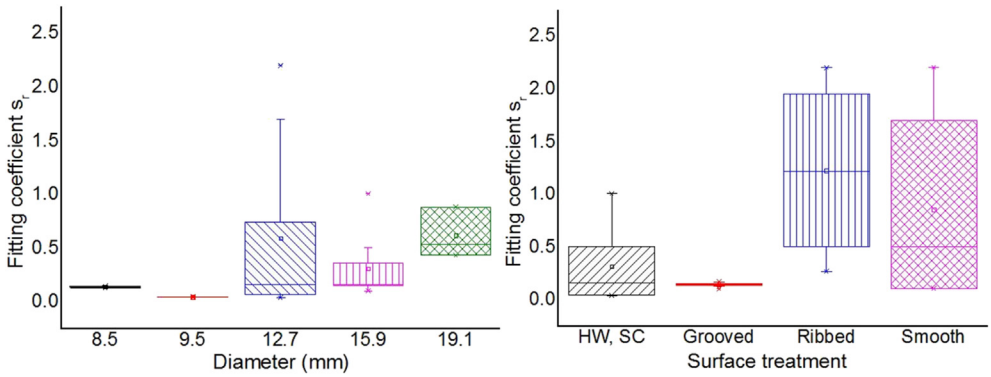

Fig. 6. Discrete conditions of fitting parameter s_r.

$$\tau_b = \frac{f_{cr}(d_{cs} + K_{tr}E_{FRP}/E_s)}{0.45\pi d_b k_1 k_4}, \tag{6}$$

where f_{cr} is the cracking strength of concrete (MPa); K_{tr} is transverse reinforcement index (mm) which is defined as $\frac{A_{tr}f_y}{10.5sn}$, where A_{tr} is the area of transverse reinforcement normal to the plane of splitting through the bars (mm^2), f_y is the yield strength of transverse reinforcement (MPa), s is the distance of center to center spacing of the transverse reinforcement (mm), n is the number of bars being developed along the plane of splitting; E_{FRP} is the modulus of elasticity of FRP bar (MPa); E_s is the modulus of elasticity of steel (MPa); k_1 is the bar location factor; k_4 is the bar surface profile factor. Thus, CSA S6-06 describes the bond strength as the function of concrete cover, concrete strength, concrete confinement provided by transverse reinforcement, bar diameter and bar surface conditions.

2.2.4. Japanese design code

The Japanese Design Code (JSCE) [19] derives the bond strength of FRP bars to concrete, mainly from the modification of the expression for steel bars, which is limited to splitting failure as given by Eqn. (4) in ACI 440.1R-06:

$$\tau_b = f_{bod}/\alpha_1, \tag{7a}$$

where α_1 is a confinement modification factor defined in the following:

$$\begin{aligned} &\alpha_1 = 1.0 \text{ for } k_c \le 1.0;\\ &\alpha_1 = 0.9 \text{ for } 1.0 < k_c \le 1.5;\\ &\alpha_1 = 0.8 \text{ for } 1.5 < k_c \le 2.0;\\ &\alpha_1 = 0.7 \text{ for } 2.0 < k_c \le 2.5;\\ &\alpha_1 = 0.6 \text{ for } k_c > 2.5. \end{aligned} \tag{7b}$$

$$k_c = \frac{c}{d_b} + \frac{15A_t}{sd_b}\frac{E_t}{E_s}, \tag{7c}$$

$$f_{bod} = \frac{0.28\alpha_2 f_c'^{2/3}}{1.3} \le 3.2\ N/mm^2, \tag{7d}$$

where c is the smaller of the bottom clear cover of the main reinforcement or half of the clear space between reinforcement being developed; A_t is the area of transverse reinforcement; s is the spacing of transverse reinforcement; E_t is the modulus of elasticity for the transverse reinforcement; E_s is the modulus of elasticity for the steel. f_{bod} is the designed bond strength of concrete; α_2 is the modification factor for bond strength (1.0 where bond strength is equal to or greater than that of deformed steel bars; otherwise value shall be reduced according to test results). It is clear that the bond strength of FRP bars defined in Japanese design code is a function of the concrete strength, the concrete cover, the concrete confinement provided by transverse reinforcement and the bar location.

2.2.5. Comparisons of national and international design specifications

National and international design specifications associated with the bond strength of GFRP bars to concrete have been discussed through Section 2.2. A comparison among these codes is summarized and listed in Table 1 to better understand the standardized language in bond strength, the factors that affect bond strength considered in the design standards, and their applicability.

It is clear that key factors such as, concrete strength, bar diameter, concrete cover and bar location are taken into account for all these standards. Embedment length is considered only in ACI 440.1R-06 standard for bond strength calculation. It is worth noting that the bar surface profile (spiral wrapped vs. helical lugged) did not appear to influence the bond strength, and it is necessary to be further investigated. Differently, more additional information for determination of bond strength, including fiber type used in reinforcement, and confinement provided by transverse reinforcement, is used in the Canadian or Japanese Codes, which is ignored in ACI 440.1R-06.

Further valuable information of these design codes, ACI 440.1R-06, CSA S806-02, CSA S6-06 and JSCE, for bond strength prediction was reported by Ametrano [48], where the beam test was used. He documented his investigation on the bond strength of GFRP bars with two different bar sizes with diameters $d_b = 15.9$ and 19.1 mm, and to four different concrete mixes, labeled as HP-S10, RYE, Duct1 and Duct2, with compression strength of 71.2, 115 (~130 MPa), 147.8 and 174.5 MPa, respectively. As clearly illustrated in Fig. 7a and b, bond strengths obtained from the tests are higher than those predicted through the four design standards, indicating that the codes is conservative, and the development length provided is sufficient for FRP bars to reach their ultimate stress prior to bond failure. Furthermore, the bond strength predicted by ACI 440.1R-06 is closer to the test results. For another, the bond strength predicted by CSA S806-02, CSA S6-06 and JSCE differ little from each other.

3. Critical factors and their impacts on failure modes and bond strength of GFRP bars to concrete

A data-driven parametric study was carried out for over 680 pullout-test specimens that were collected from the literature [1–31], [32–62], [63–93]. This database was valuable information

Table 1
Factors for determining bond strength in the national and international design codes.

Design standards	Concrete strength	Bar diameter	Concrete cover	Bar location	Embedded length	Bar surface	Transverse confinement	Fiber type
ACI 440.1R-06	✓	✓	✓	✓	✓	✓	×	×
CSA S806-02	✓	✓	✓	✓	×	✓	×	✓
CSA S6-06	✓	✓	✓	✓	×	✓	✓	✓
JSCE	✓	✓	✓	✓	×	×	✓	×

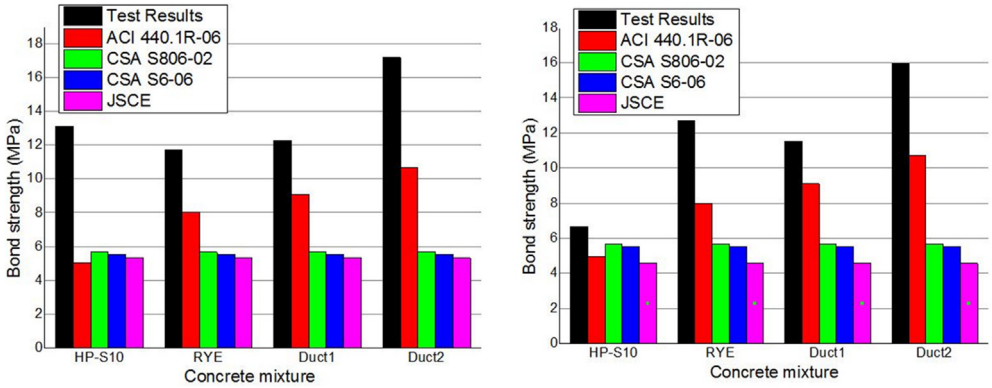

a) d_b=15.9 mm b) d_b=19.1 mm

Fig. 7. Bond strength calculated in design standards based on Ametrano's work [48].

for determining the critical factors that affect the bond behavior of GFRP bars to concrete and their corresponding failure modes and bond strength. The review demonstrated that GFRP bars to concrete commonly displays several bond failure modes, including pullout failure, splitting failure, anchorage failure, rebar fracture and peeling off of resin, while these bond failures and the bond strength are majorly associated with: concrete compressive strength, bar size, concrete cover, embedment length, bar spacing, and transverse reinforcements, as discussed in more detail below.

3.1. Failure mode and bond strength associated with concrete compressive strength

3.1.1. Failure mode

Fig. 8 was plotted to describe the relationship of the failure modes with respect to the concrete compressive strength. It is clear that both pullout and splitting failures are overwhelmingly dominant, accounting for over 80% of all the failure modes regardless of concrete strength. Specifically, pullout failure vs. concrete compressive strength displays an approximate normal distribution with a mean value of the concrete compressive strength ranging from 40 to 50 MPa. Splitting failure primarily falls into the range of the concrete compressive strength between 30 and 50 MPa. Differently, anchorage failure occurred when concrete has a higher compressive strength over 30 MPa. Rebar fracture was observed from about 32 cases that compressive strength was at 30 MPa and 50 MPa, while 42 specimens failed by peeling off of resin at higher concrete strength at levels of 50–60 MPa.

3.1.2. Bond strength

The pullout and splitting failures are two major dominant failure modes, as stated in Section 3.11. Thus, the data mining from the

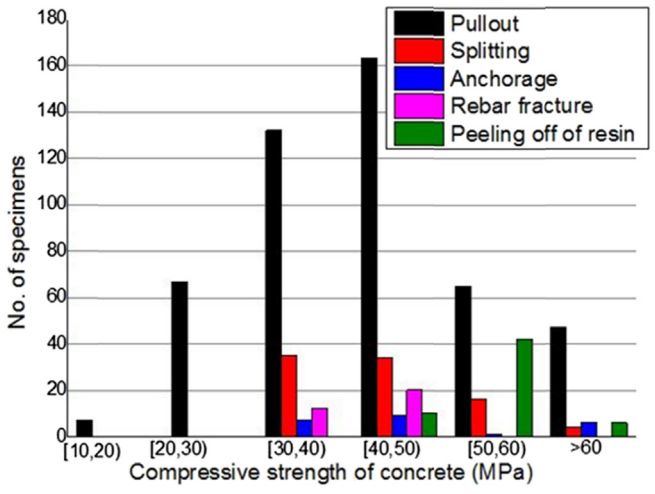

Fig. 8. Failure modes associated with concrete compressive strength.

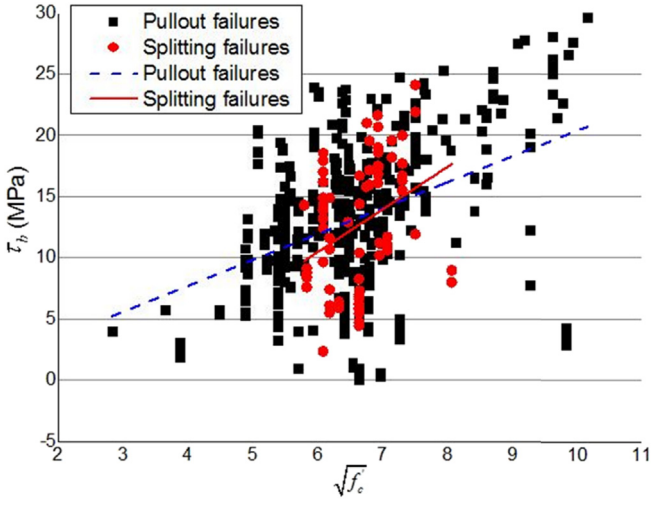

Fig. 9. Bond strength versus concrete strength $\sqrt{f'_c}$.

literature mainly aligns with these two failures. Fig. 9 displays the bond strength vs. the concrete compressive strength (in terms of $\sqrt{f'_c}$) curves of both pullout and concrete splitting, in which τ_b is the bond strength between concrete and GFRP bar, and f'_c refers to the concrete compressive strength at 28 days.

Clearly, large scatter data at both pullout and splitting failure still display the increase trendline with the increase of the concrete compressive strength, by certain proportionality to $\sqrt{f'_c}$, as observed in the literature [17,46,49,50]. It is usually GFRP bar is implemented in concrete products with a compressive strength below 55 MPa (8000 psi) [51–54], which is confirmed by heavy data points falling within 27–55 MPa shown in Fig. 9.

Davalos et al. [55] summarized the relationship between the bond strength and $\sqrt{f'_c}$. Their findings indicated that the bond strengths predicted by design codes CSA-S806 and JSCE in Section 2.23 and 2.24 are conservative, whereas ACI 440 may not be conservative when concrete compressive strength is relatively low. By using the high-strength concrete over 55 MPa (8000 psi), the bond strength predicted by ACI is more conservative than other design codes.

Note that the ratio of the bond strength to concrete strength, $\tau_b/\sqrt{f'_c}$, starts to decrease with the increase of the compressive strength after beyond 55 MPa (8000 psi) [56–58]. It is partly because higher concrete strength demands higher threshold for pulling out a bar, while the feature of high brittle for high strength concrete thus makes concrete more vulnerable to fail by coupled pullout with splitting failures. As a result, full capacity of pullout failures are less observed for high strength concrete. To clarify this statement, the bond slip, s_b, associate with the testing data in the literature is plotted against the concrete strength $\sqrt{f'_c}$, as shown in Fig. 10, where y axis is the normalized slip by s_b/l_d and l_d is the embedded length of a bar to concrete. With the increase of the compressive strength, particularly over 55 MPa (8000 psi) shown in Fig. 10, there is a significant drop in bond slip, suggesting that tests were mainly terminated by more sudden failures when concrete had a relative higher strength.

3.2. Failure mode and bond strength associated with concrete cover

3.2.1. Failure mode

Concrete cover is another critical factor that affects failure modes, bond strength and the durability of GFRP bar to concrete. Ehsani et al. [59] tested 48 GFRP bar reinforced concrete beams. Their test results indicated that specimens had splitting failures when concrete cover, c, is one time of the bar diameter ($c = 1.0\ d_b$), while pullout failures or even bar fracture were observed when concrete cover has at least twice of the bar diameter. Alves et al. [35] investigated bond characteristics of GFRP bars to concrete when subjected to environmental and loading conditions. Two different bar diameter (15.9 and 18.9 mm) and three concrete covers (1.5 d_b, 2.0 d_b and 2.5 d_b) were included in their study. The findings showed that failure modes switched from typical splitting failure to pullout failure, with the increase of concrete cover. Moreover, the study confirmed that the clear concrete cover having the value of 2.0 d_b ensure the pullout failure for 15.9-mm bar, while 2.5 d_b for the 18.9-mm bar. It implied that increasing concrete cover leads to higher confinement pressure (bearing effect) on the GFRP bars, thereby reducing the possibility of developing more cracks in the concrete surrounding the bars and thus delaying the splitting failure.

The summary of the data in the literature of concrete cover to failure modes of GFRP bar is plotted in Fig. 11, in which x axis is defined by the normalized concrete cover, c/d_b, by bar diameter d_b. As clearly illustrated in Fig. 11, particularly when the ratio of concrete cover to bar diameter is equal to or greater than four, over 400 specimens were failed by pulling out, reaching up to 60% of all over the database. Therefore, it implies that larger concrete cover provides higher confinement to the bar, thereby resulting in the more dominant pullout failure. Otherwise, splitting failure occurs prior to pullout failure when concrete cover is not sufficient to apply adequate confinement to reinforcing bars.

3.2.2. Bond strength

Fig. 12 shows the relationship of the bond strength (normalized by $\tau_b/\sqrt{f'_c}$) with concrete cover (c/d_b). High scatter data points account for high variation during tests, including varying specimen preparation, test conditions, methods and operational variation. There is still a basic increasing trendline with the increase of concrete cover, as illustrated in Fig. 12. This trend is more clearly observed if test data are more comparable. For example, Aly et al. [60] tested six full-scale beams reinforced with GFRP bars to investigate the effects of concrete cover on their bond strength, and they observed that the specimens had an increase in bond strength by approximately 27%, as concrete cover increased from one to four times of the bar diameter. Clearly, sufficient concrete cover confines GFRP bar and allows the bar to develop higher bearing force, thereby resulting in the higher bond strength to concrete.

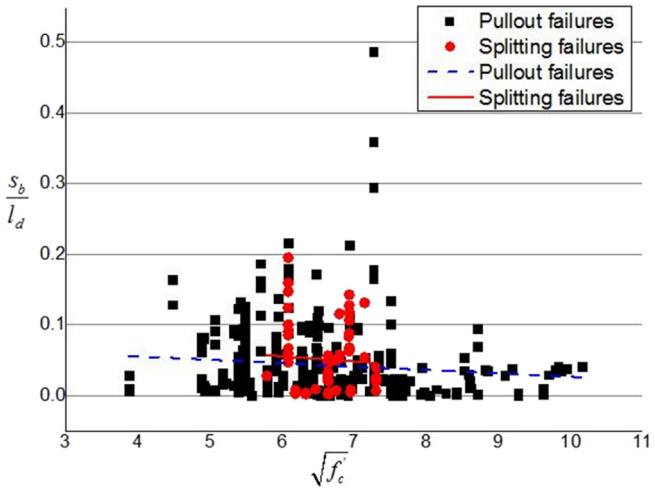

Fig. 10. Normalized bond slip versus strength $\sqrt{f'_c}$.

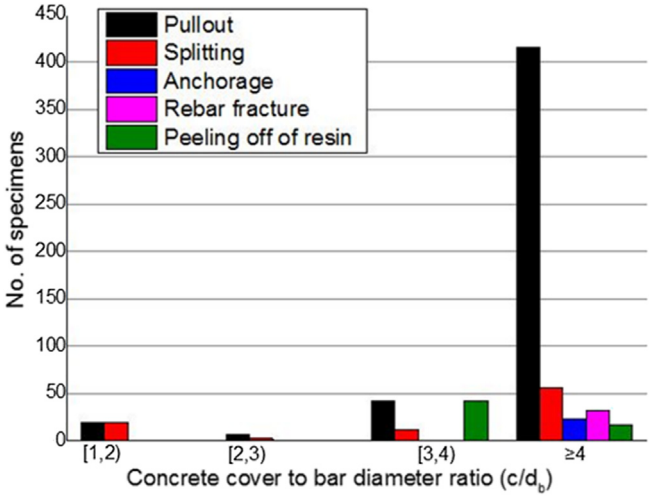

Fig. 11. Failure mode associated with concrete cover.

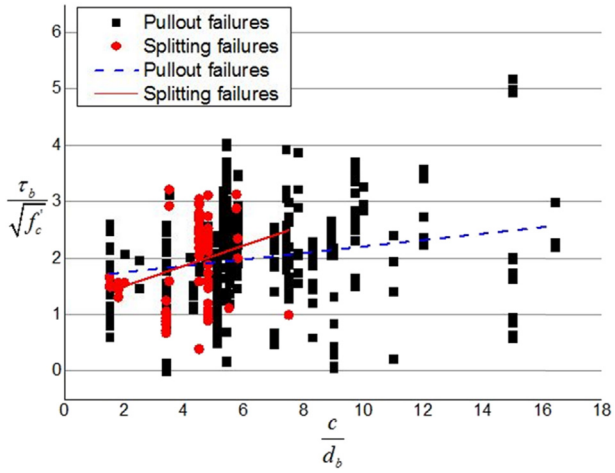

Fig. 12. Normalized bond strength versus c/d_b.

In addition, further information is gained from the correlation between the bond slip (s_b/l_d) and concrete cover (c/d_b), as shown in Fig. 13. The slip decreased when concrete cover increased as expected. Also, the trendline of splitting failure (in solid lines) has a higher gradient than that of pullout failure, indicating that increasing concrete cover provide higher confinement, which prevents development of slip movement, and thus more likely fails by a sudden energy release.

3.3. Failure mode and bond strength associated with embedment length

3.3.1. Failure mode

Similar to concrete cover, embedment length, l_d, is one of critical parameters that influence the bond strength of FRP bar to concrete. Fig. 14 is plotted for the testing data associated with both pullout and splitting failures. Pullout failure dominates the failure modes, while approximately yielding a normal distribution with a mean value ranging from 5 to 6 (times of l_d/d_b). Such embedment (5–6 times of bar size d_b) responds for total amount of 256 specimens failed by pulling out, 54% of overall failure modes. It also implies that the embedment length having five times of bar diameter enables to provide desirable bond pullout failure for GFRP bar to concrete.

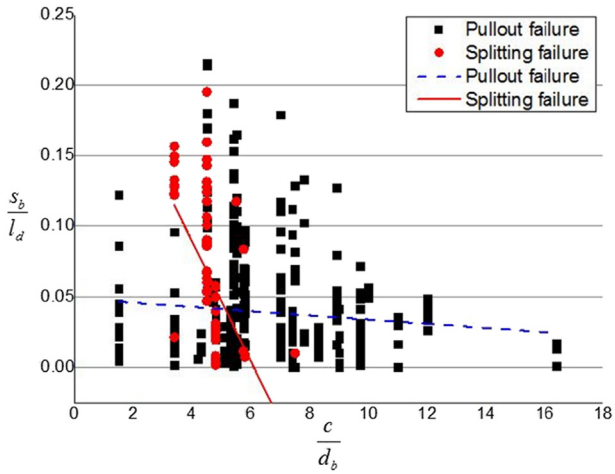

Fig. 13. Normalized bond slip versus c/d_b.

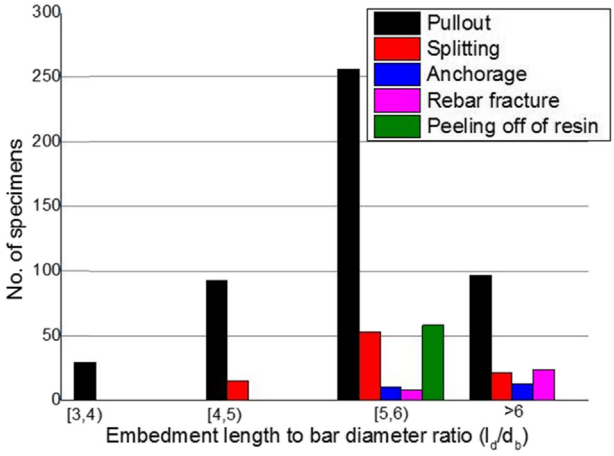

Fig. 14. Failure mode associated with embedment length.

3.3.2. Bond strength

Fig. 15 plots the normalized bond strength vs. the normalized embedment length (l_d/d_b) under both pullout and splitting failures. The maximum average bond stress of GFRP bars to concrete, illustrated in Fig. 15, decreases as the embedment length increases, similar to the previous observations for steel bars [7,11,46,49,50,61]. It is mainly due to a nonlinear distribution of the bond stress along the reinforcing bar, as schematically shown in an inserted plot in Fig. 15. As the embedment length increases, the stress yields the high unevenly distributed over a longer length, thereby resulting in the decrease in average bond stress. The identical conclusion can be drawn from the ACI 440 1R-06 in Section 2.2.1 and also most single cases confirm this observation. For example, Achillides et al. [11] reported that the increase of the embedment length not only leads to the decrease of the maximum average developed bond stress of FRP bars, but also yields the lower initial bond stiffness accordingly, which responds for high nonlinearly non-uniform distribution of the bond stress along the longer bar.

On the other hand, the bond slip increased as the embedment increased, as shown in Fig. 16. The longer embedded length yields relatively higher applied force, while the longer length provides the longer "strain" length to develop deformation when subjected to higher applied force, and thus failure frequently occurs at the larger slip.

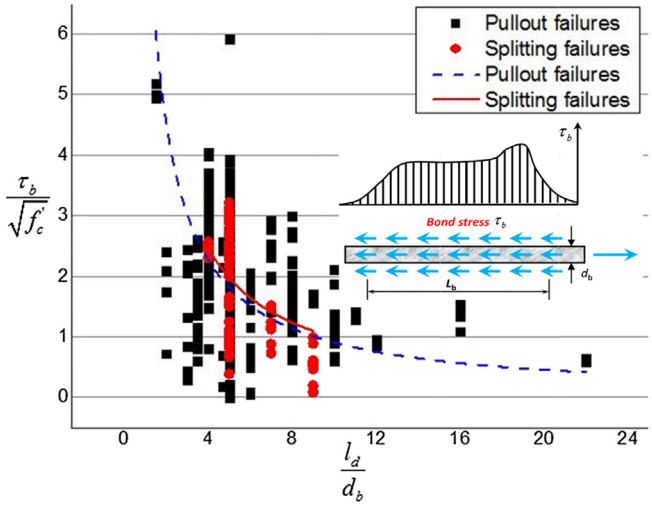

Fig. 15. Normalized bond strength versus l_d/d_b.

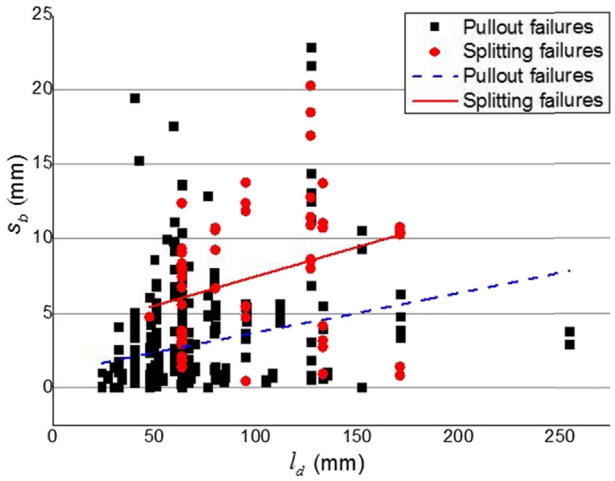

Fig. 16. Bond slip versus l_d.

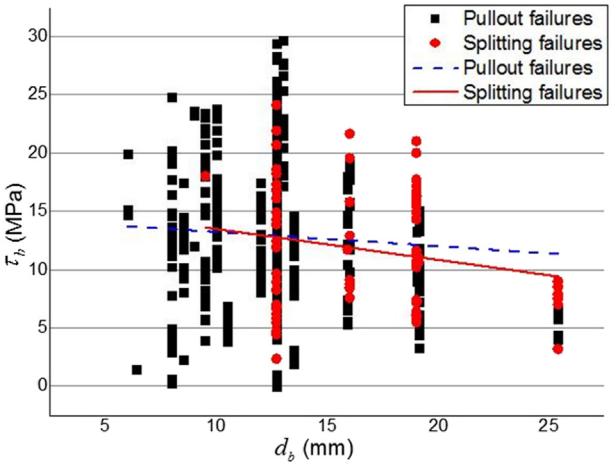

Fig. 18. Bond strength versus d_b.

3.4. Failure mode and bond strength associated with bar diameter

3.4.1. Failure mode

Fig. 17 presents the failure types with respect to the bar diameter. Even though there is no clear correlation between bar size and failure modes, pullout and splitting failures are still major failures through different bar size. Pullout failures respond for 500 out of 682 cases, in particular at bar diameter of 12–14 mm. It seems that there are increasing splitting failures as the increase of bar diameter, while other three failure modes were observed far less frequently, with 23 specimens for anchorage failure; 32 specimens for rebar fracture and 53 specimens for peeling off of resin.

3.4.2. Bond strength

Fig. 18 shows the relationship of bond strength (τ_b) with bar diameter (d_b). It is clear that the bond strength decreased as the bar diameter increased for both pullout and splitting failures. It is partially because the increased bar diameter leads to the increased contact area with concrete, while naturally trap the void or other defects at the interface during concrete cast and construction [35,62,63], thereby statistically causing the higher possibility to form weak interface between the bar and concrete, and ultimately reducing to the lower average bond strength.

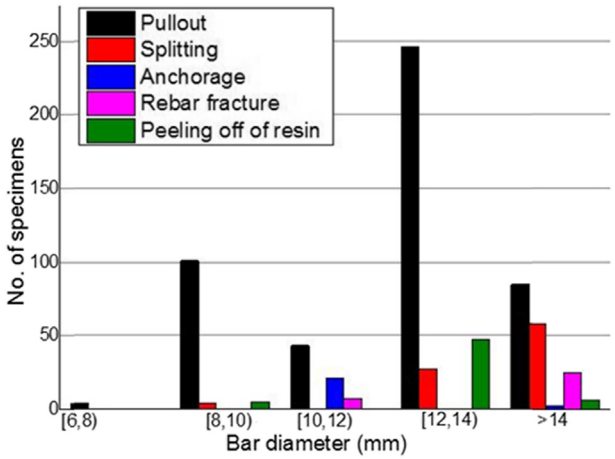

Fig. 17. Failure modes associated with bar diameter.

3.5. Failure mode and bond strength associated with bar surface conditions

3.5.1. Failure mode

Bar surface conditions in terms of ribbed, helically wrapped, sand coated, helically wrapped or sand coated are commonly used in direct pullout tests. Smooth surface is normally taken as a reference to quantify the effects of various surface treatments on bond behavior and failure modes. Fig. 19 demonstrates the relationships between surface conditions and failure modes. Failure modes and surface conditions are assigned with the legends, as shown in Fig. 19. For simplicity, the first term of the legends used represents the failure modes, while the second term is for surface conditions: a) R = ribbed; b) HW = helically wrapped; c) SC = sand coated; d) HWSC = helically wrapped and sand coated; e) SW = spirally wrapped.

Clearly, the pullout failure mode are over 84% of all cases, while the ribbed FRP bars (Pullout-R) occupied the largest proportion among all surface treatments, with about 35% of total failures. Helically wrapped and sand coated surface of GFRP bar (P-HW-SC) and P-HW are the second and third better surfaces to allow desirable mechanical interlocking, taking up about 22% and 13%, respectively. There are only 16% splitting failures, while similarly to its counterpart, helically wrapped and sand coated or ribbed surfaces are the major treatments. These surface conditions provide higher mechanically interlocking, which leads to relatively higher hoop stress and hence results in splitting failures.

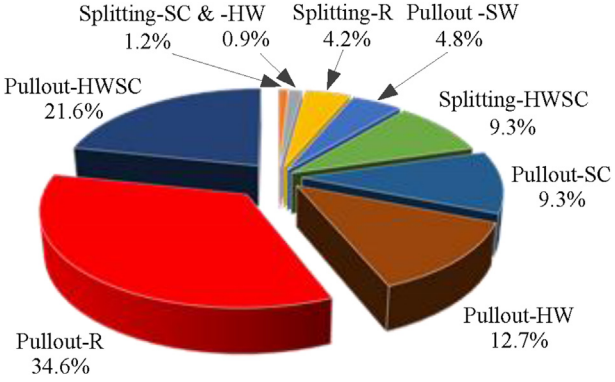

Fig. 19. Two failure modes associated with varying bar surface conditions.

3.5.2. Bond strength

FRP bar is manufactured to different deformed surface patterns, such as ribbed/lugged, indented, sand coated and spirally wrapped. The ACI 440.1R-06 states that surface textures of the FRP bar plays an important role in bond mechanism to concrete, even though no specific variable is included in the existing ACI code to account for the contribution. The CSA S806-02 specifies a coefficient factor (i.e., 1.0 for surface roughed or sand coated or braided surface; 1.05 for spiral pattern surfaces or ribbed surfaces; 1.8 for indented surfaces) for different bar surfaces for determining the development length of FRP bars.

Till now, there still remain opposite opinions about the effects of bar surfaces on the bond strength, as reported by different researchers. Wambeke et al. [22] summarized tests of 269 beam-type specimens, and concluded that bar surfaces have no effects on the bond strength of FRP bars to concrete. This was agreed with Mosley et al. [64] who reported the identical conclusions based upon their beam splice tests for bond behaviors of both GFRP and AFRP bars. Differently, Baena et al. [47] performed 88 direct pullout tests for FRP bars, suggesting that surface treatments appear to influence the bond strength significantly. Also, Hao et al. [65] studied the ribbed GFRP bars with different rib height and spacing. Their findings showed that the surface macrotexture has high impact on the bond behavior, failure modes and the bond strength of GFRP bars to concrete.

3.6. Failure mode and bond strength associated with enhancement of concrete from transverse reinforcement confinement or fiber-reinforced concrete matrix

3.6.1. Enhancement from transverse reinforcement confinement

Transverse reinforcement provides confinement to concrete, which not only delays the splitting cracking but also changes the failure modes and bond-slip relationship by relatively higher ductile performance, thus increasing the bond strength and bond slip of reinforcing bars to concrete. With the help of the transverse reinforcement, as stated in the ACI 408R-06, the concrete is confined to prevent or delay a splitting failure, and thus it will develop higher bond stress to the bar and likely fail by bar pulling out.

On the other hand, some researchers, including Wambeke et al. [22], pointed out that such confinement from transversal reinforcement may not increase the average bond stress of FRP bar effectively. Steel bar has apparent ribs and thus the transverse reinforcement can effectively apply higher bearing force on the steel ribs to develop the higher bond strength. However, the argument for FRP bar lies in the fact that a relative lower rib area in FRP bar may lead to relatively weaker bearing force, even though there is transverse reinforcement.

3.6.2. Enhancement from fiber-reinforced concrete matrix

Discrete fibers are usually used to mix in concrete, referred to fiber reinforced concrete, to enhance concrete tensile strength and toughness. Recently, fiber reinforced concrete has been accepted to improve bond behavior in FRP bar to concrete [66–74]. Plizzari [66] and Harajli et al. [67] reported that fibers increased the splitting bond strength and improved the ductility of bond failure as compared to plain concrete. Wang and Belarbi [70,71] investigated bond strength of GFRP and CFRP bars in both plain and fiber reinforced concrete when exposed to aggressive environments, including freeze-thaw cycles, and salt solutions. They found that the polypropylene fibers in concrete matrix significantly improved the bond capacity and their durability. The fiber-reinforce concrete specimens after environmental exposure only had a 6% reduction in ultimate bond strength, as compared to 28% reduction for plain concrete counterparts. Enhancement of the bond behavior and bond strength in fiber reinforced concretes are attributed to the restriction effects of polypropylene fibers to prevent and delay the crack development and propagation at both environmental exposure and direct pullout tests. Kim et al. [72] investigated 63 cubic fiber-reinforced-concrete specimens with GFRP bars embedded in them and concluded that with fiber addition (steel, PP and PVA fibers) in concrete, both bond strength and crack development are significantly enhanced. Ding et al. [73] reported that the bond capacity of GFRP bars in concrete reinforced by hybrid fibers (both steel fibers and polypropylene fibers), was appeared to show equivalent or better performance than that of steel bars in concrete. Furthermore, the hybrid use of different fibers demonstrated significant influence on the post-peak bond behavior of GFRP bars in concrete matrix.

3.7. Failure mode and bond strength associated with bar casting position

ACI 440.1R-06 states that bond strength of horizontal FRP bar, in particular at top location, may experience a high decrease in bond strength and thus a modification factor is stipulated for accounting for the location, similar to the identical requirements for determining the development length of reinforcing steel bar (in ACI 318-14). Previous tests from the literature [59] revealed that the top-cast bars had an approximately 66% decrease in bond strength as compared to that of the bottom-cast bars. Chaallal and Benmokrane [38] investigated 3 bar diameters (No. 4–6) and recommended that the top-cast bar modification factor ranged from 1.08 to 1.38 for normal-strength concrete, while 1.11 to 1.22 for high-strength concrete. This modification factor was further revised through more tests by Wambeke and Shield [22], and use 1.5 for top-cast bars in ACI 440.1R-06, while 1.3 given in CSA S806-02.

4. Environmental conditions and their impacts on bond behavior and bond strength of FRP bars

4.1. Freeze-thaw cycles

Damage in concrete due to freeze-thaw cycles relies on the saturation of concrete. Freezing-thaw cycles have minimum adverse effects on dry concrete, even under a relative humidity to 75–80% [75]. Experience shows that accumulated damage in concrete are frequently observed [76,77], however, when the concrete is partially or fully saturated with freezing water or deicing chemicals. There still remain opposite opinions about the impacts of freeze-thaw cycles on FRP bar bond strength. Mashima et al. [49] investigated bond behavior of CFRP, GFRP and AFRP bars to concrete when subjected to freeze-thaw cycles. The pullout test, they found that CFRP and GFRP bars performed well after the freezing and thawing cycle, without obvious reduction in bond capacity. However, the AFRP bar specimens lost about 40% bond strength after 600 freezing and thawing cycles. Micelli and Nanni [30] studied CFRP and GFRP bars to concrete exposed to 200 freeze-thaw cycles. They found that freeze-thaw cycles combined with humidity did not degrade the specimens. Similar conclusions were also observed from other researchers [34]. Uomoto et al. [78] studied the effect of freezing and thawing on FRP bars by immersing FRP bars in a freeze-thaw water chamber over 300 cycles, indicating that the effects of freeze-thaw cycles are only limited to the surface of FRP material. Strength reduction of FRP bars was only within 8%.

On the other hand, Won and Park [36] documented their study on GFRP bars to concrete under 300 freeze-thaw cycles. Their results stated that approximately 20% reduction in bond resistance was observed. The reason is that the water permeates through the voids (or new developed microcracks) in concrete matrix, while the

growth of ice crystals during repeated freezing process generate high pressure to concrete, thus leading to microcracks in concrete. As a result, this will break down the interface between concrete and GFRP bar. Presence of concrete cracks also yields a low confinement to GFRP bar and thus causes less bond strength. Moreover, accumulated micro-/macro-cracks in concrete during the freezing and thawing cycles may allow other chemical solution to easily penetrate to concrete matrix, and even easily degrade GFRP bar when penetrating through the interface, ultimately resulting in bar strength loss and the bond strength reduction.

It is clear that the freeze-thaw damage to concrete may be affected by complex interaction of numerous factors, including concrete permeability, temperature gradient, and air void systems. Alves et al. [35] tested GFRP bars embedded in concrete under sustained and fatigue loading conditions. Their results even supported that freeze-thaw cycles enhanced the bond strength between sand-coated GFRP bar and concrete by approximately 40%.

4.2. Wet-dry cycles

Wet-dry cycles are usually related to freeze-thaw cycles or solution conditions [30]. Sen et al. [79] investigated durability of S-2 glass/epoxy pretensioned beams exposed to wet-dry cycles in a 15% salt solution. They reported that GFRP bars lost their effectiveness after 6 months for the precracked beams and 15 months for the uncracked beams.

Almusallam et al. [80] carried out experiment tests of concrete beams reinforced with GFRP bars when subjected to different certain stress levels. After wet-dry conditioning, there were significant loss in tensile strength of GFRP bars when subjected to sustained loads of 20–25% ultimate strength, about 27–29% after 4 months, 37–47% after 8 months and 47–55% after 16 months. Ahmed et al. [81] tested 90 concrete specimens with sand-coated GFRP reinforcing bars, which were subjected to 25 wet-dry cycles. The test results indicated that the bond strength and anchorage capacity of GFRP bars reduced over time when exposed to wet-dry cycles, which was also confirmed to the prediction by ACI-349-85.

4.3. Alkaline solutions

Concrete has a high alkalinity with a pH value ranging from 10.5 to 13.5, while GFRP reinforcements embedded in concrete tend to degrade under high alkaline environment [82,83]. Studies about effect of alkaline environment on FRP materials can be traced back to 1990's. Cowley and Robertson [84] studied the effect of the pH and temperature on GFRP composite in sodium hypochlorite solutions. The results showed that GFRP bar degraded proportionally with the increase of temperature over time after 4-month exposure to solutions with variable pH values (7–7.75, 8 to 8.85, 9 to 9.5, 10 to 10.5 and 11 to 11.5) under the temperature 99 °C. Tannous and Saadatmanesh [85] tested 160 bar samples and 10 concrete beams to evaluate the durability of AR glass bars. The specimens were exposed to solutions with the pH of 12 at temperature of 25 and 60 °C, respectively. Significant loss of strength of AR glass bars was observed, indicating AR glass did not improve resistance in alkaline concrete environment. Also, similar studies related to alkali attack to GFRP bars were conducted by many researchers [30,33,86–89]. Chen et al. [26] conducted five types of solutions to simulate environmental conditions for both bare FRP (GFRP and CFRP) bars and FRP-concrete elements. Solution 1 was tap water to simulate high humidity. Solution 2 was made with a pH value of 13.6 to simulate the pore solution of normal concrete, while solution 3 with a pH value of 12.7 was aimed for high-performance concrete. Solution 4 consisted of sodium chloride (NaCl) and sodium sulfate (Na2SO4) was to simulate ocean water. Solution 5 included sodium chloride (NaCl) and potassium hydroxide (KOH) with a pH value of 13, and was to simulate concrete pore solution with chloride from deicing salts. In addition, elevated temperatures of 40 and 60 °C were employed to accelerate the test process. The results showed that GFRP bars failed with separation of fibers and rupture of fiber bundle. A reduction of 4% for CFRP bars and 36% for GFRP bars in tensile strength were observed in solution 2 at 60 °C. Furthermore, bond strength of GFRP bars to concrete decreased by approximately 12%. Alkali attacks to GFRP bars may have more severe adverse effects on the GFRP bar reinforced concrete durability, as compared to the impacts of wet-dry and freeze-thaw cycles.

On the other hand, the work undertaken by ISIS Canada [90] on the long-term full size tests of RC structures over ten years claimed that the GFRP flexural tension reinforcing bars are durable and highly compatible with concrete material in field structures [91–93]. Those engineering structures were exposed to natural environmental conditions including de-icing salt, freeze-thaw and wet-dry cycles, thermal range from −35 °C to 35 °C for a duration of five to eight years. A set of analytical approaches such as Scanning Electron Microscopy (SEM), Energy Dispersive X-ray (EDX), Optical Microscopy (OM), Fourier Transformed Infrared Spectroscopy, were used to monitor and detect the degradation state of GFRP material. Different from laboratory test conclusions, there was no obvious degradation of the GFRP reinforcements. Particularly, the manufacturing process in terms of the curing ratio (96% or above) is of central importance to ensure the resin system to resist the chemical attack and avoid moisture absorption.

4.4. High temperatures

The Coefficient of thermal expansion (CTE) of steel bars in concrete is similar to surrounding concrete. Thus, there are negligible stresses built up in the interface between steel and concrete, when subjected to thermal loading. However, GFRP reinforcements (with resins) have much larger CTE, as compared to concrete. Accordingly, when ambient temperature vibrates, GFRP bar reinforced concrete may experience high thermal stresses, ultimately resulting in splitting cracks [94,95].

Glass fibers have high reliable mechanical properties under high temperature up to 250 °C [96]. Polymer resins (e.g., vinyl ester and polyester resins) in GFRP bar may, however, turn soft with high viscoelasticity, but with decreasing mechanical performance (strength and stiffness), if ambient temperature reaches up to or even over the glass transition temperature [97]. Also the resins may experience failures, such as matrix hardening, microcracking and fiber-matrix debonding when exposed to sub-zero temperature [98]. Kumahara et al. [99] conducted high-temperature tests of FRP bars and reported that there was a reduction of about 20% in the tensile strength for CFRP and GFRP bars at a temperature of 250 °C, and about 60% for AFRP bars. It was expected that failure may occur firstly in resin matrix rather than fibers. Similar conclusions of tensile strength loss was also observed by Alsayed et al. [100].

Katz et al. [101,102] investigated the GFRP bar bond behavior in concrete in terms of bond strength, pre-peak and post-peak performance under the temperature ranging from 20 to 250 °C. It appeared to have an 80–90% reduction in bond strength. The load-slip curve exhibited two different stages. At the first stage prior to pre-peak, the load-slip curve has a gradually decreasing slope as temperature increased. It implied that the GFRP bar stiffness decrease with the increase of the temperature. At the second stage (post-peak), the slope decreased moderately at elevated temperature (200–250 °C) than that at room temperature (20 °C). It mainly because of a weakened wedging effect of GFRP bar to concrete at elevated temperature [101,102]. Identical results were observed by Wang et al. [103] and Carvelli et al. [104].

By use of this thermal feature in GFRP bar, high temperature is often implemented as accelerated testing to predict long-term (75- to 100-year) durability of FRP bar reinforced concrete [26,27,32,105].

5. Conclusions

This paper presented an overall review of bond behavior of GFRP bar to concrete, and the associated durability. Some conclusions can be drawn as follows:

1. There are still no universal analytical models that can be applicable to general bond-slip behavior of GFRP bar to concrete. BPE modified model and CMR model have relatively simple form and reliable results that can be applied to investigate bond stress-slip process. The fitting parameters, α, β and s_r, specified in these two models are generated based on the literature, and the suggested values are classified based on different bar diameters and surface treatments, if tests data are not available.
2. Bond strength of GFRP to concrete has been specified in the national and international design codes and is summarized to ensure engineers to better understand their applicability. Comparisons between different design standards regarding bond strength prediction show that four key factors, including concrete strength, bar diameter, concrete cover and bar location, are taken into account in all these standards. Embedment length is considered only in ACI 440 standard for bond strength calculation. Differently, more information (bar surface profile, fiber type used in reinforcement, and confinement provided by transverse reinforcement) is considered in the Canadian or Japanese Codes, which is ignored in ACI 440. Moreover, the equations regarding bond strength provided in ACI 440 is specific to splitting failure and hence, formula for pullout failure needs to be developed for general purpose.
3. Over 600 pullout-test specimens were mined from the literature and presented a comprehensive parametric study from a statistical point of view. All data supported that pullout and splitting failures are overwhelmingly dominant over all of the failure modes. Factors that affect the bond behavior, failure modes and bond strength of GFRP bar to concrete are identified and quantitatively plotted for ensuring engineers to fully understand their impacts. Specifically, bond strength has linear relationships with critical factors: a) concrete compressive strength; b) concrete cover; and c) bar size. There is a nonlinear relationship between the bond strength and embedment length. Moreover, discrete fiber or transverse reinforcement is accepted as an effective solution to increase the bond strength of GFRP bar to concrete.
4. Bond degradations under environmental conditions, such as freezing-thawing cycling, wet-dry cycling, alkaline solutions and high temperature are summarized. Environmental damage to concrete may be affected by complex interaction of numerous factors. Thus, there still remain opposite opinions in the effects of environmental conditions, such as freeze-thaw and wet-dry cycles, on the bond strength. Some studies revealed that alkaline solution or high temperature leads to significant loss of both tensile and bond strength. Future studies are required to determine the combined environmental effects.

Acknowledgment

The authors gratefully acknowledge the financial support provided by 1) ND NASA (EPSCoR FAR0023941), 2) ND NSF EPSCoR (FAR0022364), and 3) US DOT (FAR0025913). The results, discussion, and opinions reflected in this paper are those of the authors only and do not necessarily represent those of the sponsor. In addition, thanks to the great information and support from Hughes Brother Inc.

References

[1] Committee, A. Guide for the design and construction of structural concrete reinforced with FRP bars. ACI 440.1 R 2006:6.
[2] Bedard C. Composite reinforcing bars: assessing their use in construction. Concr Int 1992;14(1):55–9.
[3] Koch GH, Brongers MP, Thompson NG, Virmani YP, Payer JH. Corrosion cost and preventive strategies in the United States. 2002.
[4] French C. Durability of concrete structures. Struct Concr 2003;4(3):101–7.
[5] Saadatmanesh H, Ehsani MR. Application of fiber-composites in civil engineering. In: Structural materials. ASCE; 1989.
[6] Ballinger CA. Development of composites for civil engineering. in. In: Advanced Composites Materials in Civil Engineering Structures. ASCE; 1991.
[7] Nanni A, Al-Zaharani M, Al-Dulaijan S, Bakis C, Boothby I. 17 bond of FRP reinforcement to concrete-experimental results. In: Non-metallic (FRP) Reinforcement for Concrete Structures: Proceedings of the Second International RILEM Symposium. CRC Press; 1995.
[8] Nanni A, De Luca A, Zadeh HJ. Reinforced Concrete with FRP Bars: Mechanics and Design. CRC Press; 2014.
[9] Brown VL, Bartholomew CL. FRP reinforcing bars in reinforced concrete members. ACI Mater J 1993;90(1).
[10] Pecce M, Manfredi G, Realfonzo R, Cosenza E. Experimental and analytical evaluation of bond properties of GFRP bars. J Mater Civ Eng 2001;13(4):282–90.
[11] Achillides Z, Pilakoutas K. Bond behavior of fiber reinforced polymer bars under direct pullout conditions. J Compos Constr 2004;8(2):173–81.
[12] Yan F, Lin Z. New strategy for anchorage reliability assessment of GFRP bars to concrete using hybrid artificial neural network with genetic algorithm. Compos Part B Eng 2016;92:420–33.
[13] Faza SS, GangaRao HV. Bending and bond behavior of concrete beams reinforced with plastic rebars. Transp Res Rec 1991;1290.
[14] Daniali S. Development length for fiber-reinforced plastic bars. In: Advanced Composite Materials in Bridges and Structures. Sherbrooke: Canada; 1992.
[15] Shield C, French C, Retika A. Thermal and mechanical fatigue effects on GFRP rebar-concrete bond. In: Proceedings of the 3rd International Symposium on Non-metallic (FRP) Reinforcement for Concrete Structures (FRPRCS-3), Sapporo; 1997.
[16] DeFreese JM, Roberts-Wollmann CL. Glass fiber reinforced polymer bars as top mat reinforcement for bridge decks. 2002.
[17] Okelo R, Yuan RL. Bond strength of fiber reinforced polymer rebars in normal strength concrete. J Compos Constr 2005;9(3):203–13.
[18] Lee J-Y, Kim T-Y, Kim T-J, Yi C-K, Park J-S, You Y-C, et al. Interfacial bond strength of glass fiber reinforced polymer bars in high-strength concrete. Compos Part B Eng 2008;39(2):258–70.
[19] Machida A, Uomoto T. Recommendation for design and construction of concrete structures using continuous fiber reinforcing materials, vol. 23. Research Committee on Continuous Fiber Reinforcing Materials, Japan Society of Civil Engineers; 1997.
[20] Association, C.S. Design and construction of building components with fibre-reinforced polymers. Canadian Standards Association; 2002.
[21] Association, C.S. Canadian highway bridge design code. Canadian Standards Association; 2006.
[22] Wambeke BW, Shield CK. Development length of glass fiber-reinforced polymer bars in concrete. ACI Struct J 2006;103(1).
[23] Masmoudi A, Masmoudi R, Ouezdou MB. Thermal effects on GFRP rebars: experimental study and analytical analysis. Mater Struct 2010;43(6):775–88.
[24] Masmoudi R, Masmoudi A, Ouezdou MB, Daoud A. Long-term bond performance of GFRP bars in concrete under temperature ranging from 20 C to 80 C. Constr Build Mater 2011;25(2):486–93.
[25] Yoo D-Y, Kwon K-Y, Park J-J, Yoon Y-S. Local bond-slip response of GFRP rebar in ultra-high-performance fiber-reinforced concrete. Compos Struct 2015;120:53–64.
[26] Chen Y, Davalos JF, Ray I, Kim H-Y. Accelerated aging tests for evaluations of durability performance of FRP reinforcing bars for concrete structures. Compos Struct 2007;78(1):101–11.
[27] Belarbi A, Wang H. Bond durability of FRP bars embedded in fiber-reinforced concrete. J Compos Constr 2011;16(4):371–80.
[28] Mijovic J. Interplay of physical and chemical aging in graphite/epoxy composites. J Compos Mater 1985;19(2):178–91.
[29] Tuttle M. A framework for long-term durability predictions of polymeric composites. Rotterdam: Progress in Durability Analysis of Composite Systems; 1996. p. 196–176.
[30] Micelli F, Nanni A. Durability of FRP rods for concrete structures. Constr Build Mater 2004;18(7):491–503.
[31] Charles R. The strength of silicate glasses and some crystalline oxides. In: ICF0, Swampscott-MA (USA) 1959; 2012.

[32] Gonenc O. Durability and service life prediction of concrete reinforcing materials. UNIVERSITY OF WISCONSIN-MADISON; 2003.
[33] Abbasi A, Hogg PJ. Temperature and environmental effects on glass fibre rebar: modulus, strength and interfacial bond strength with concrete. Compos Part B Eng 2005;36(5):394–404.
[34] Koller R, Chang S, Xi Y. Fiber-reinforced polymer bars under freeze-thaw cycles and different loading rates. J Compos Mater 2007;41(1):5–25.
[35] Alves J, El-Ragaby A, El-Salakawy E. Durability of GFRP bars' bond to concrete under different loading and environmental conditions. J Compos Constr 2010;15(3):249–62.
[36] Won J-P, Park C-G, Lee S-J, Hong B-T. Durability of hybrid FRP reinforcing bars in concrete structures exposed to marine environments. Int J Struct Eng 2013;4(1–2):63–74.
[37] Committee, A. Bond and Development of Straight Reinforcing Bars in Tension (ACI 408R-03). Detroit, Michigan, US: American Concrete Institute; 2003.
[38] Chaallal O, Benmokrane B. Pullout and bond of glass-fibre rods embedded in concrete and cement grout. Mater Struct 1993;26(3):167–75.
[39] Cosenza E, Manfredi G, Realfonzo R. Behavior and modeling of bond of FRP rebars to concrete. J Compos Constr 1997;1(2):40–51.
[40] Pepe M, Mazaheripour H, Barros J, Sena-Cruz J, Martinelli E. Numerical calibration of bond law for GFRP bars embedded in steel fibre-reinforced self-compacting concrete. Compos Part B Eng 2013;50:403–12.
[41] Eligehausen R, Popov EP, Bertero VV. Local bond stress-slip relationships of deformed bars under generalized excitations. 1982.
[42] Malvar LJ. Bond stress-slip characteristics of FRP rebars. DTIC Document; 1994.
[43] Lin X, Zhang Y. Evaluation of bond stress-slip models for FRP reinforcing bars in concrete. Compos Struct 2014;107:131–41.
[44] Cosenza E, Manfredi G, Realfonzo R. 20 analytical modelling of bond between FRP reinforcing bars and concrete. In: Non-metallic (FRP) Reinforcement for Concrete Structures: Proceedings of the Second International RILEM Symposium. CRC Press; 1995.
[45] Antonietta Aiello M, Leone M, Pecce M. Bond performances of FRP rebars-reinforced concrete. J Mater Civ Eng 2007;19(3):205–13.
[46] Benmokrane B, Tighiouart B. Bond strength and load distribution of composite GFRP reinforcing bars in concrete. ACI Mater J 1996;93(3).
[47] Baena M, Torres L, Turon A, Barris C. Experimental study of bond behaviour between concrete and FRP bars using a pull-out test. Compos Part B Eng 2009;40(8):784–97.
[48] Ametrano D. Bond characteristics of glass fibre reinforced polymer bars embedded in high performance and ultra-high performance concrete. Toronto, Ontario, Canada: Ryerson University; 2011. p. 1–132.
[49] Makitani E, Irisawa I, Nishiura N. Investigation of bond in concrete member with fiber reinforced plastic bars. ACI Special Publication; 1993. p. 138.
[50] Tighiouart B, Benmokrane B, Gao D. Investigation of bond in concrete member with fibre reinforced polymer (FRP) bars. Constr Build Mater 1998;12(8):453–62.
[51] Tepfers R. A theory of bond applied to overlapped tensile reinforcement splices for deformed bars. Chalmers University of Technology Goteborg; 1973.
[52] Orangun C, Jirsa J, Breen J. A reevaulation of test data on development length and splices. In: ACI Journal Proceedings. ACI; 1977.
[53] Darwin D, McCabe SL, Idun EK, Schoenekase SP. Development length criteria: bars not confined by transverse reinforcement. ACI Struct J 1992;89(6).
[54] Esfahani MR, Rangan BV. Local bond strength of reinforcing bars in normal strength and high-strength concrete (HSC). ACI Struct J 1998;95(2).
[55] Davalos JF, Chen Y, Ray I. Long-term durability prediction models for GFRP bars in concrete environment. J Compos Mater 2012;46(16):1899–914.
[56] Azizinamini A, Stark M, Roller JJ, Ghosh S. Bond performance of reinforcing bars embedded in high-strength concrete. ACI Struct J 1993;90(5).
[57] Zuo J. Bond strength of high relative rib area reinforcing bars. 1999.
[58] Zuo J, Darwin D. Splice strength of conventional and high relative rib area bars in normal and high-strength concrete. ACI Struct J 2000;97(4).
[59] Ehsani M, Saadatmanesh H, Tao S. Bond of GFRP rebars to ordinary-strength concrete. ACI Special Publication; 1993. p. 138.
[60] Aly R. Stress along tensile lap-spliced fibre reinforced polymer reinforcing bars in concrete. Can J Civ Eng 2007;34(9):1149–58.
[61] Fava G, Carvelli V, Pisani MA. Remarks on bond of GFRP rebars and concrete. Compos Part B Eng 2016;93:210–20.
[62] De Larrard F, Shaller I, Fuchs J. Effect of the bar diameter on the bond strength of passive reinforcement in high-performance concrete. ACI Mater J 1993;90(4).
[63] Quayyum S. Bond behaviour of fibre reinforced polymer (FRP) rebars in concrete. 2010.
[64] Mosley CP, Tureyen AK, Frosch RJ. Bond strength of nonmetallic reinforcing bars. ACI Struct J 2008;105(5).
[65] Hao Q, Wang Y, He Z, Ou J. Bond strength of glass fiber reinforced polymer ribbed rebars in normal strength concrete. Constr Build Mater 2009;23(2):865–71.
[66] Plizzari G. Bond and splitting crack development in normal and high strength fiber reinforced concrete. In: 13th Engrg mechanics Division Conference—EMD99, Baltimore (MD, USA), on CD; 1999.
[67] Harajli M, Hamad B, Karam K. Bond-slip response of reinforcing bars embedded in plain and fiber concrete. J Mater Civ Eng 2002;14(6):503–11.
[68] Won J-P, Park C-G, Kim H-H, Lee S-W, Jang C-I. Effect of fibers on the bonds between FRP reinforcing bars and high-strength concrete. Compos Part B Eng 2008;39(5):747–55.
[69] Dancygier AN, Katz A, Wexler U. Bond between deformed reinforcement and normal and high-strength concrete with and without fibers. Mater Struct 2010;43(6):839–56.
[70] Wang H, Belarbi A. Ductility characteristics of fiber-reinforced-concrete beams reinforced with FRP rebars. Constr Build Mater 2011;25(5):2391–401.
[71] Wang H, Belarbi A. Flexural durability of FRP bars embedded in fiber-reinforced-concrete. Constr Build Mater 2013;44:541–50.
[72] Kim B, Doh J-H, Yi C-K, Lee J-Y. Effects of structural fibers on bonding mechanism changes in interface between GFRP bar and concrete. Compos Part B Eng 2013;45(1):768–79.
[73] Ding Y, Ning X, Zhang Y, Pacheco-Torgal F, Aguiar J. Fibres for enhancing of the bond capacity between GFRP rebar and concrete. Constr Build Mater 2014;51:303–12.
[74] Yang J-M, Min K-H, Shin H-O, Yoon Y-S. Effect of steel and synthetic fibers on flexural behavior of high-strength concrete beams reinforced with FRP bars. Compos Part B Eng 2012;43(3):1077–86.
[75] 201, A.C.. Guide to durable concrete. In: ACI Journal Proceedings. ACI; 1977.
[76] Fursa TV, Utsyn GE, Korzenok IN, Petrov MV. Using electric response to mechanical impact for evaluating the durability of the GFRP-concrete bond during the freeze-thaw process. Compos Part B Eng 1 April 2016;90:392–8.
[77] Yun H-D. Effect of accelerated freeze–thaw cycling on mechanical properties of hybrid PVA and PE fiber-reinforced strain-hardening cement-based composites (SHCCs). Compos Part B Eng 2013;52:11–20.
[78] Uomoto T, Mutsuyoshi H, Katsuki F, Misra S. Use of fiber reinforced polymer composites as reinforcing material for concrete. J Mater Civ Eng 2002;14(3):191–209.
[79] Sen R, Mariscal D, Shahawy M. Durability of fiberglass pretensioned beams. ACI Struct J 1993;90(5).
[80] Almusallam TH, Al-Salloum YA. Durability of GFRP rebars in concrete beams under sustained loads at severe environments. J Compos Mater 2006;40(7):623–37.
[81] Ahmed EA, El-Salakawy EF, Benmokrane B. Tensile capacity of GFRP post-installed adhesive anchors in concrete. J Compos Constr 2008;12(6):596–607.
[82] Won J-P, Lee S-J, Kim Y-J, Jang C-I, Lee S-W. The effect of exposure to alkaline solution and water on the strength–porosity relationship of GFRP rebar. Compos Part B Eng 2008;39(5):764–72.
[83] Al-Salloum YA, El-Gamal S, Almusallam TH, Alsayed SH, Aqel M. Effect of harsh environmental conditions on the tensile properties of GFRP bars. Compos Part B Eng 2013;45(1):835–44.
[84] Cowley T, Robertson M. Effect of pH and temperature on fiberglass-reinforced composites in sodium hypochlorite solutions. Mater Perform 1991;30(7):46–9.
[85] Tannous FE, Saadatmanesh H. Durability of AR glass fiber reinforced plastic bars. J Compos Constr 1999;3(1):12–9.
[86] Benmokrane B, Wang P, Ton-That TM, Rahman H, Robert J-F. Durability of glass fiber-reinforced polymer reinforcing bars in concrete environment. J Compos Constr 2002;6(3):143–53.
[87] Nkurunziza G, Debaiky A, Cousin P, Benmokrane B. Durability of GFRP bars: a critical review of the literature. Prog Struct Eng Mater 2005;7(4):194–209.
[88] Kim H-Y, Park Y-H, You Y-J, Moon C-K. Short-term durability test for GFRP rods under various environmental conditions. Compos Struct 2008;83(1):37–47.
[89] Zhou J, Chen X, Chen S. Effect of different environments on bond strength of glass fiber-reinforced polymer and steel reinforcing bars. KSCE J Civ Eng 2012;16(6):994–1002.
[90] ISIS Canada. ISIS Canada, D.M.N., Strengthening Reinforcing Concrete Structures with Externally Bonded Fiber Reinforced Polymers. Canadian Network of Centers of Excellence on Intelligent Sensing for Innovative Structures. Winnipeg, Manitoba, Canada: ISIS Canada Corporation; 2001.
[91] Mufti AA, Rizkalla S, Canada I. Reinforcing Concrete Structures with Fibre Reinforced Polymers [computer File]. 2001 [ISIS Canada].
[92] Mufti A, Onofrei M, Benmokrane B, Banthia N, Boulfiza M, Newhook J, et al. Durability of GFRP reinforced concrete in field structures. In: Proceedings of the 7th International Symposium on Fiber-reinforced Polymer Reinforcement for Reinforced Concrete Structures (FRPRCS-7), Kansas City, Mo; 2005.
[93] Mufti A, Benmokrane B, Boulfiza M, Bakht B, Breyy P. Field study on durability of GFRP reinforcement. In: International Bridge Deck Workshop, Winnipeg, Manitoba, Canada; 2005.
[94] Masmoudi R, Zaidi A, Gérard P. Transverse thermal expansion of FRP bars embedded in concrete. J Compos Constr 2005;9(5):377–87.
[95] Galati N, Nanni A, Dharani LR, Focacci F, Aiello MA. Thermal effects on bond between FRP rebars and concrete. Compos Part A Appl Sci Manuf 2006;37(8):1223–30.
[96] Yamasaki Y, Masuda Y, Tanano H, Shimizu A. Fundamental properties of continuous fiber bars. ACI Spec Publ 1993:138.
[97] Fried JR. Polymer science and technology. Pearson Education; 2014.
[98] Karbhari V, Chin J, Hunston D, Benmokrane B, Juska T, Morgan R, et al. Durability gap analysis for fiber-reinforced polymer composites in civil infrastructure. J Compos Constr 2003;7(3):238–47.

[99] Kumahara S, Masuda Y, Tanano H, Shimizu A. Tensile strength of continuous fiber bar under high temperature. ACI Special Publication; 1993. p. 138.
[100] Alsayed S, Al-Salloum Y, Almusallam T, El-Gamal S, Aqel M. Performance of glass fiber reinforced polymer bars under elevated temperatures. Compos Part B Eng 2012;43(5):2265–71.
[101] Katz A, Berman N, Bank LC. Effect of high temperature on bond strength of FRP rebars. J Compos Constr 1999;3(2):73–81.
[102] Katz A. Bond mechanism of FRP rebars to concrete. Mater Struct 1999;32(10):761–8.
[103] Wang Y, Wong P, Kodur V. An experimental study of the mechanical properties of fibre reinforced polymer (FRP) and steel reinforcing bars at elevated temperatures. Compos Struct 2007;80(1):131–40.
[104] Carvelli V, Pisani MA, Poggi C. High temperature effects on concrete members reinforced with GFRP rebars. Compos Part B Eng 2013;54:125–32.
[105] Robert M, Benmokrane B. Effect of aging on bond of GFRP bars embedded in concrete. Cem Concr Compos 2010;32(6):461–7.